Research Article

Farouk Omar Hamdoon, Enass H. Flaieh, and Alaa Abdulhady Jaber*

Numerical investigations of two vibrating cylinders in uniform flow using overset mesh

https://doi.org/10.1515/cls-2022-0208
received March 17, 2023; accepted June 28, 2023

Abstract: In this research, flow around two vibrating cylinders in a tandem arrangement is simulated at Reynolds number Re = 200 using the dynamic overset mesh technique in finite volume-based commercial software. This investigation aims to study the combined influences of the spacing between the two identical circular cylinders and their excitation frequency in the flow. The cylinders are excited by a transverse forced vibration in a uniform cross-flow by applying a simple harmonic motion. The gap distance between the vibrating cylinders is chosen to be L/D = 1.5 and 4, and the vibration amplitude is kept constant at A/D = 0.25. The study focuses on three frequency ratios of the cylinders' excitation frequency to Strouhal shedding frequency of the single stationary cylinder f_e/f_s = 0.8, 1.0, and 1.2. Simulation results showed that the flow characteristics over the two vibrating circular cylinders differ from that of a single vibrating cylinder. Also, it is observed that the lock-in state (resonance) for the two vibrating cylinders and the vortex wake patterns are highly affected by the gap distance between cylinders and the excitation frequency.

Keywords: cylinder vibration, overset mesh, fast Fourier transform, vibration

1 Introduction

Flow around a group of vibrating cylinders in various arrangements is of great importance in numerous engineering applications, such as chimneys, heat exchanger tubes, transmission lines, suspension bridge cables, and offshore piles. The interaction effect between the multi-vibrating cylinders and the vortex wake is more complex than that of flow over a single vibrating cylinder. However, to investigate the flow characteristics around multi-vibrating cylinders, it is necessary to study the flow behavior around a single vibrating cylinder.

The flow around a single oscillating circular cylinder was experimentally investigated by Bishop and Hassan [1], Koopmann [2], and Tanida *et al.* [3]; and numerically by Meneghini and Bearman [4], Nobari and Naderan [5], Placzek *et al.* [6], and Kumar *et al.* [7]. These studies were conducted over a wide range of transverse excitation frequencies of cylinders. It was concluded that at a certain range of excitation frequencies, a phenomenon termed "lock-in" (resonance) occurs, where the vortex shedding frequency deviates from that of a corresponding stationary cylinder f_s (Strouhal shedding frequency) and becomes synchronized with the cylinder excitation frequency f_e. The lock-in phenomenon can increase the vibrating response of the structures leading to fatigue failure. Williamson and Roshko [8] extensively examined the different vortex shedding modes behind a single vibrating cylinder. The study classified the wake mode into three groups: 2S mode, in which a single vortex is formed on each side of the cylinder per cycle; 2P mode, in which a pair of vortices appears on each side per cycle; and P + S mode, where a pair of vortices and a single vortex are formed alternately per cycle. In comparison with a circular cylinder, the vibrating square or triangular cylinders show different flow characteristics since the separation points starts at the sharp edges [9,10].

The flow behavior over two stationary cylinders is another important study to understand the flow characteristics around the multiple vibrating cylinders. There are different configurations to place two cylinders adjacent to one another. The tandem configuration is the simplest arrangement of two circular cylinders. Zdravkovich [11] and Igarashi [12] have studied flow characteristics over two stationary cylinders arranged in a tandem configuration. The experimental results found that a change in flow patterns around the two cylinders occurs at a specific spacing and Reynolds number. Numerical simulations have been performed on two stationary cylinders at Reynolds

* **Corresponding author: Alaa Abdulhady Jaber,** Mechanical Engineering Department, University of Technology - Iraq, Baghdad, Iraq, e-mail: alaa.a.jaber@uotechnology.edu.iq
Farouk Omar Hamdoon: College of Engineering, Wasit University, Wasit, Iraq
Enass H. Flaieh: Mechanical Engineering Department, University of Technology - Iraq, Baghdad, Iraq

number Re = 100 by Li *et al.* [13], Mittal *et al.* [14], and Sharman *et al.* [15], and at Reynolds number Re = 200 by Slaouti and Stansby [16], Meneghini *et al.* [17], and Borazjani and Sotiropoulos [18]. Among the other configurations of two cylinders is the side-by-side arrangement, where the wake patterns are highly affected by gap spacing and Reynolds number [17,19,20].

The flow characteristics of the two transversely vibrating cylinders differ from that of two fixed cylinders and a single vibrating cylinder. Studies concerning vibrating circular cylinders in a tandem arrangement are relatively rare. Mahir and Rockwell [21] investigated experimentally the flow past two transversely vibrating circular cylinders in a tandem arrangement at Re = 160 and at two spacing ratios L/D = 2.5 and 5 (L is the spacing distance between the centers of the cylinders and D is the diameter of the cylinders). The results showed that the vibration of the two cylinders results in a broader lock-in band than that noticed for a single vibrating cylinder. Later, Papaioannou *et al.* [22] conducted a numerical investigation to examine the geometry of Arnold's tongue (the geometry of lock-in regions on an amplitude–frequency diagram). It was observed that holes in Arnold's tongue could be seen in the case of two vibrating circular cylinders in contrast with that of a single vibrating cylinder with a solid Arnold's tongue.

The objective of the present study is to investigate the flow characteristics around two vibrating circular cylinders compared to a baseline case of a single vibrating cylinder. The two circular cylinders in the tandem arrangement are forced to vibrate transversely to a uniform cross-flow at Re = 200, implementing the dynamic overset mesh approach in computational fluid dynamics (CFD) code ANSYS FLUENT 19.0. The excitation frequency and the spacing between the two cylinders are chosen as essential parameters for the current investigation.

This article is organized as follows: Section 2 deals with the numerical technique where the governing equations, the computational domain, and the overset mesh are presented. In Section 3, the presented numerical model is validated by simulating the flow around a single fixed circular cylinder and two fixed circular cylinders. Section 4 discusses the simulation results of the flow past a single vibrating cylinder and two vibrating cylinders in a tandem arrangement. Finally, the conclusions and summary are given in Section 5.

2 Computational method

In this section, the governing equations of the flow field and the numerical model implemented with a commercial CFD code are illustrated.

2.1 Governing equations

For the two-dimensional laminar incompressible flow, the governing equations can be expressed by a set of continuity and momentum equations as follows:

$$\frac{\partial u}{\partial x} + \frac{\partial v}{\partial y} = 0, \tag{1}$$

$$\frac{\partial u}{\partial t} + \frac{\partial u^2}{\partial x} + \frac{\partial (uv)}{\partial y} = -\frac{\partial p}{\partial x} + \frac{1}{\mathrm{Re}}\left[\frac{\partial^2 u}{\partial x^2} + \frac{\partial^2 u}{\partial y^2}\right], \tag{2}$$

$$\frac{\partial v}{\partial t} + \frac{\partial (uv)}{\partial x} + \frac{\partial v^2}{\partial y} = -\frac{\partial p}{\partial y} + \frac{1}{\mathrm{Re}}\left[\frac{\partial^2 v}{\partial x^2} + \frac{\partial^2 v}{\partial y^2}\right], \tag{3}$$

where the velocity components along x and y directions are u and v, respectively; p is the pressure; ρ is the fluid density, μ is the dynamic viscosity; Re represents the Reynolds number $\left(\mathrm{Re} = \frac{\rho UD}{\mu}\right)$, where D is the cylinder diameter and U is the free-stream velocity. In the present study, the numerical parameters are set to adopt fixed Reynolds number Re = 200 for all computations. The cylinders are excited to oscillate transversely to the incoming flow according to a simple harmonic motion as follows:

$$Y(t) = A\sin(2\pi f_e t), \tag{4}$$

where $Y(t)$ is the cylinder oscillation in a cross-flow direction, A is the vibration amplitude of the cylinders, f_e is the excitation frequency derived from the frequency ratio f_e/f_s, where f_s is the Strouhal shedding frequency of the single stationary cylinder.

A finite volume-based commercial software ANSYS FLUENT 19.0 is used to solve the governing equations for the flow field. The incompressible Navier–Stokes equations are discretized using the finite volume method , where the integral form of the conservation equations are solved numerically for control volumes which form a partition of the computational domain (for more details, see ref. [23]). The transverse vibration of the two cylinders is implemented with the user-defined function tool integrated with the flow solver. A COUPLED algorithm is implemented for the incompressible flow to solve the pressure–velocity coupled equations. The first-order implicit scheme is implemented for the unsteady terms in the momentum equation. The second-order upwind scheme is implemented for convective terms. Time step sizes are restricted to Δt = 0.0025 s in all numerical computations.

2.2 Computational domain and overset mesh

The schematic diagram of the computational domain adopted in the present study is illustrated in Figure 1.

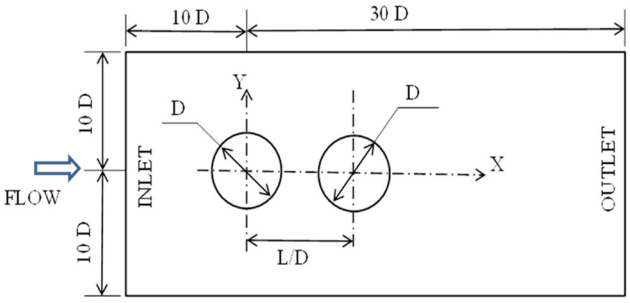

Figure 1: The computational domain.

Two transversely vibrating cylinders of identical diameter are placed in a rectangular domain $40D \times 20D$, where D is the diameter of the cylinders. The upstream cylinder is placed such that the center is $10D$ away from the inlet boundary, while the downstream cylinder is located such that the spacing distance between the centers of cylinders is $L/D = 1.5$ and 4, respectively. The cylinders are applied to no-slip boundary conditions, while the lower and upper boundary conditions are of slip-wall type. The boundary of inflow is set to have free stream velocity. The outflow boundary is set to have pressure at a reference value of zero.

The dynamic overset mesh technique in ANSYS FLUENT 19.0 is used to perform numerical simulation on the flow around the two vibrating circular cylinders. This technique allows to build multiple separate meshes, one for each region of the problem and combines them into one complete domain [24,25]. In the current study, three individual meshes are created: the rectangular grid consists of 27,787 cells, and another two cylindrical grids are the moving component meshes consisting of 7,214 cells for each. The rectangular grid represents the static background mesh, while the moving component meshes, with outer diameter $2D$ and inner diameter D, are assigned to attach to the two vibrating cylinders. Hence, the two cylinders oscillate without any mesh deformation along the fluid domain. The overset static background mesh and the two moving component meshes are illustrated in Figure 2.

3 Numerical validation

The current numerical technique is validated by performing simulations on two different test cases for which benchmark results have been reported in the literature.

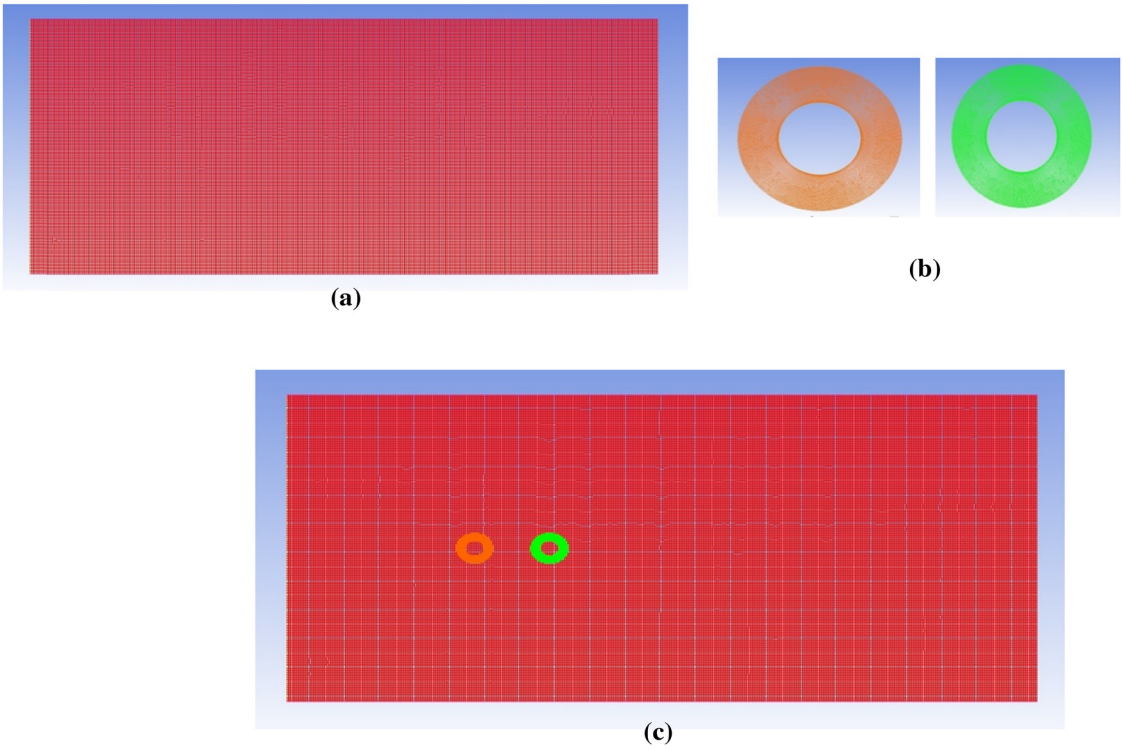

Figure 2: Overset mesh for the flow past two tandem cylinders. (a) Static background mesh, (b) two moving component meshes, and (c) component meshes are embedded in the background mesh.

The first flow test case around a single fixed circular cylinder is simulated at Re = 200. The time history of the drag coefficients (C_d) and lift coefficients (C_l) is depicted in Figure 3. The Fourier's transformations of the lift coefficients' time history yield to St = f_sD/U (Strouhal number) of about 0.195, as shown in Figure 4. The vorticity field around the fixed cylinder and the wake are depicted in Figure 5. Highly similar findings are observed in comparison with the numerical simulations using different methods presented by Meneghini *et al.* [17] and Zhou *et al.* [26].

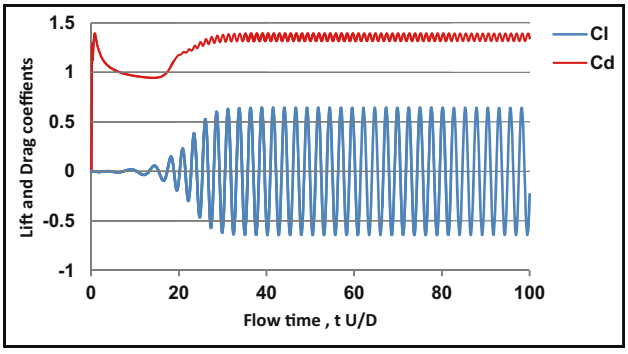

Figure 3: Force coefficients' time history of the single fixed cylinder at Re = 200.

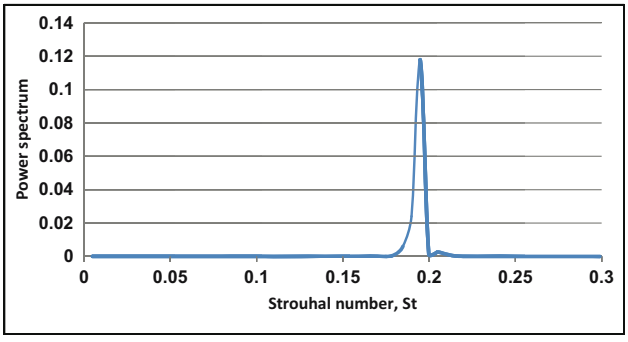

Figure 4: Strouhal number of the single fixed cylinder at Re = 200.

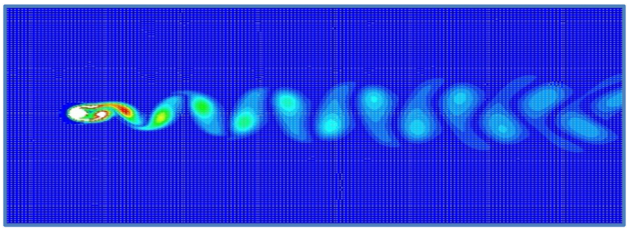

Figure 5: Instantaneous vorticity field over the single fixed cylinder.

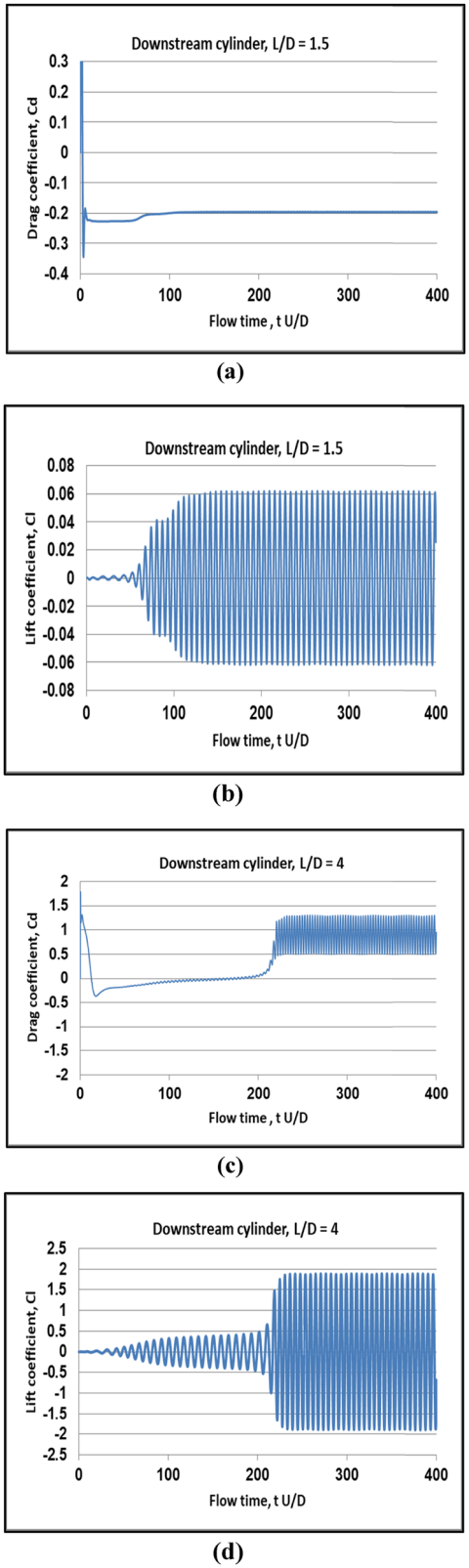

Figure 6: Force coefficients' time history of the downstream cylinder at Re = 200. (a) Drag coefficient for L/D = 1.5, (b) lift coefficient for L/D = 1.5, (c) drag coefficient for L/D = 4, and (d) lift coefficient for L/D = 4.

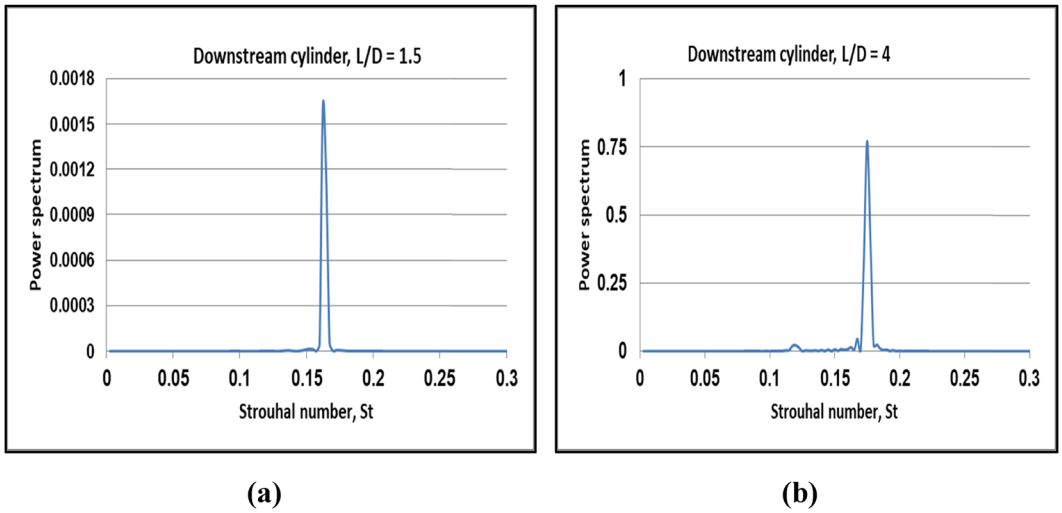

(a) (b)

Figure 7: Strouhal numbers of the downstream cylinder at Re = 200. (a) L/D = 1.5 and (b) L/D = 4.

The second test case of flow around two fixed circular cylinders is simulated to confirm the accuracy of the current numerical approach in modeling the flow interference over cylinders in proximity to one another. Two identical circular cylinders in a tandem arrangement are simulated at Re = 200 for a spacing distance of L/D = 1.5 and L/D = 4 between the upstream and downstream cylinders. This test case was studied using different numerical methods by Slaouti and Stansby [16], Meneghini *et al.* [17], and Borazjani and Sotiropoulos [18]. The force coefficients' time history and the Strouhal numbers for the downstream cylinders are plotted in Figures 6 and 7.

The Strouhal numbers are lower than that computed for the case of a single cylinder, where St = 0.165 for spacing L/D = 1.5 and St = 0.174 for spacing L/D = 4, as can be seen in Figure 7. The present computation results are in good agreement with the results published in the literature.

Different flow configurations are observed at various spacing between the two cylinders, as depicted in Figure 8. When the spacing distance is L/D = 1.5 (Figure 8a), the separating shear layer from the upstream cylinder does not have enough space, and thus there are no apparent vortices shedding from the upstream cylinder. However, as the spacing distance increases to L/D = 4 (Figure 8b), the vortices are shed from both the upstream and downstream cylinders.

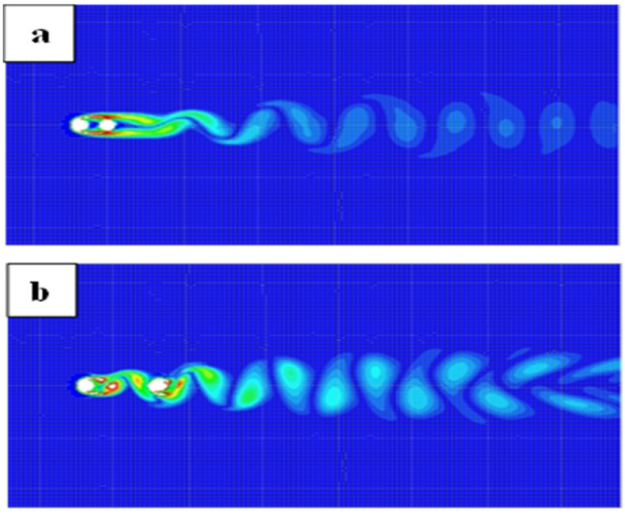

Figure 8: Instantaneous vorticity fields over the two fixed cylinders. (a) L/D = 1.5 and (b) L/D = 4.

4 Results and discussions

The computations of the flow over single and two vibrating cylinders are performed in this section. The numerical results of the lock-in state (resonance) and wake patterns at three frequency ratios are compared and discussed.

4.1 Single vibrating cylinder

A uniform flow around a single vibrating circular cylinder is simulated at Re = 200 to establish a baseline for comparison purposes. A numerical simulation is carried out to investigate the influence of different vibration frequencies with constant amplitude A/D = 0.25 on the lift and drag forces acting on a single cylinder. The study focuses on determining the lock-in state, in which the vortex shedding frequency is

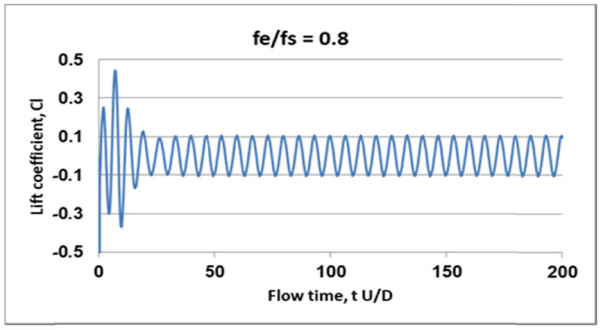

(a)

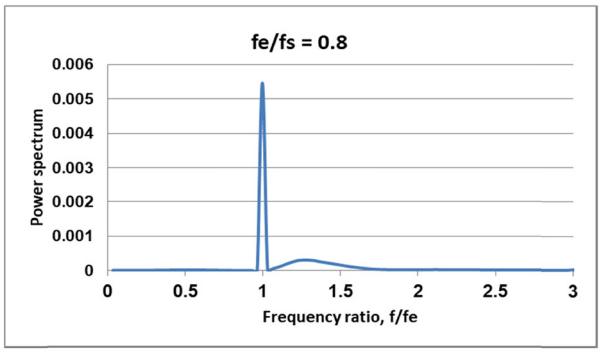

(b)

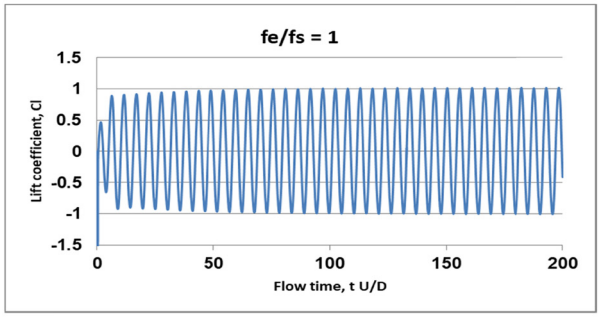

(c)

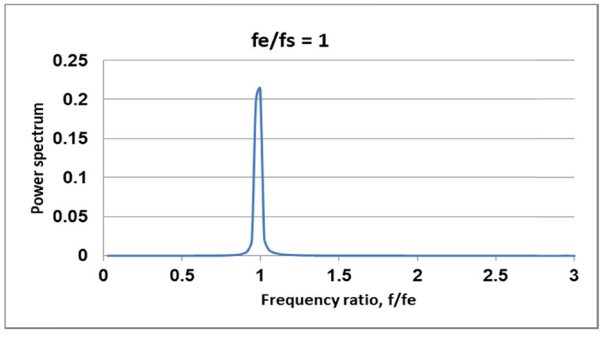

(d)

Figure 9: Lift coefficients' time history and power spectrum diagram of the single vibrating cylinder at Re = 200. (a) and (b) for f_e/f_s = 0.8, (c) and (d) for f_e/f_s = 1.0, and (e) and (f) for f_e/f_s = 1.2.

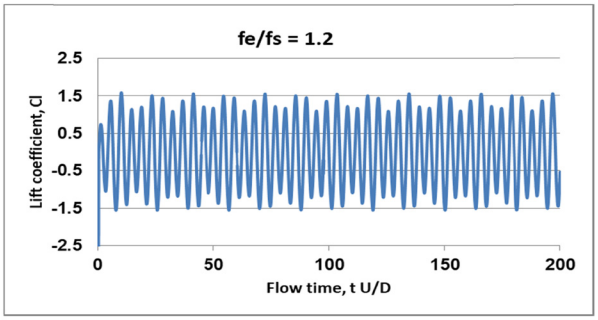

(e)

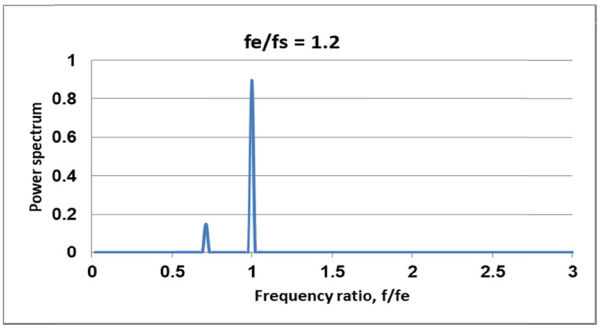

(f)

Figure 9: (*Continued*)

dominated by the forced excitation frequency f_e completely rather than controlled by the Strouhal shedding frequency of a corresponding fixed cylinder f_s. Computations are performed on a single cylinder forced to vibrate at varying frequency ratios f_e/f_s = 0.8, 1.0, and 1.2.

Figure 9a–d shows that the lock-in state occurs for two cases of f_e/f_s = 0.8 and 1.0. It can be observed that the lift coefficients' time history is absolutely periodic and purely sinusoidal. The power spectrum diagram of the lift coefficients clearly depicts that the dominant frequency is the excitation frequency f_e (lock-in state), where only one dominant peak at f/f_e = 1.0 appears, indicating that the excitation frequency f_e controls the lift forces. Figure 9e and f shows the no lock-in state for the case of f_e/f_s = 1.2. As can be seen, the time history of lift coefficients is no longer purely sinusoidal but exhibits a beating response. The power spectrum of the lift coefficients depicts two peaks: the primary peak at f_e and the secondary peak at f_m (modulation frequency). In general, the present results are consistent with the observations of Meneghini and Bearman [4], confirming the present technique's efficiency and accuracy for modeling the flow around a single vibrating cylinder at Re = 200.

The vorticity fields over the vibrating single cylinder are depicted in Figure 10. For the lock-in state, vortices in

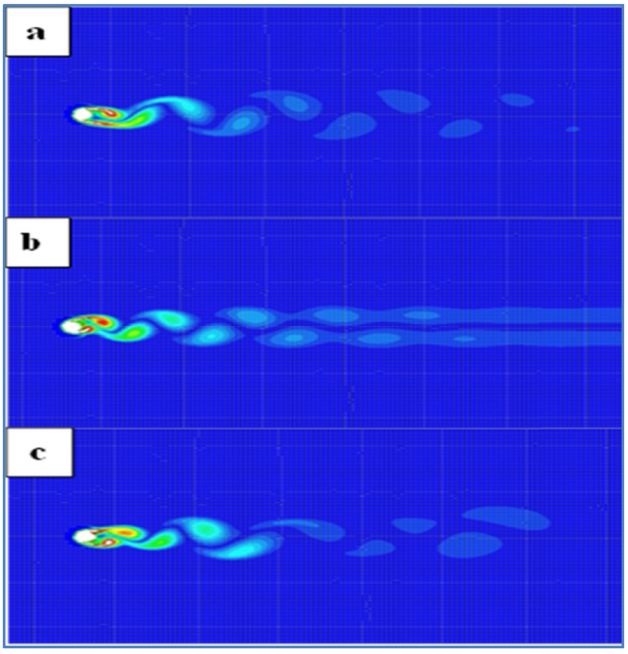

Figure 10: Instantaneous vorticity fields over the single vibrating cylinder. (a) f_e/f_s = 0.8, (b) f_e/f_s = 1.0, and (c) f_e/f_s = 1.2.

the wake at f_e/f_s = 0.8 (Figure 10a) are arranged regularly and display 2S mode where two single vortices of opposite circulation are shed per cycle. In contrast, as the frequency ratio increases to f_e/f_s = 1.0, the near wake displays 2S mode, while the positive and negative vortices in the far wake form two parallel row 2S* mode, as shown in Figure 10b. For no lock-in state at f_e/f_s = 1.2 (Figure 10c), the vortices in the wake are 2S mode with irregular arrangement due to the multiple frequency contents in the lift force time history.

4.2 Two vibrating cylinders

Computations are performed on the flow around two vibrating circular cylinders in a tandem arrangement at Re = 200. Both cylinders are forced to vibrate transversely in phase at frequency ratios f_e/f_s = 0.8, 1.0, and 1.2, while their vibration amplitude is kept at A/D = 0.25. As illustrated previously, two different spacing between the cylinders are considered in this study (L/D = 1.5 and 4).

For the case of small spacing L/D = 1.5, the lock-in state occurs at all frequency ratios f_e/f_s = 0.8, 1.0, and 1.2. As can be noticed from Figure 11, the time histories of lift coefficients are purely sinusoidal at different frequency ratios for the downstream cylinder. Only one dominant peak can be observed in the power spectrum

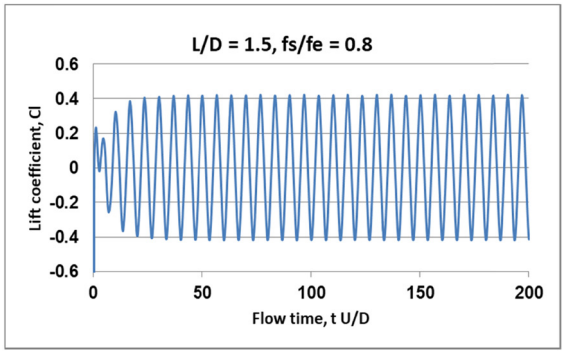

(a)

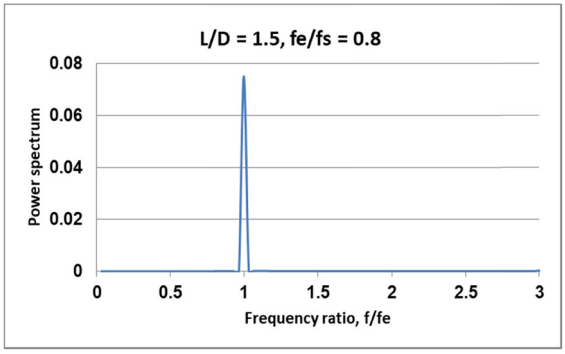

(b)

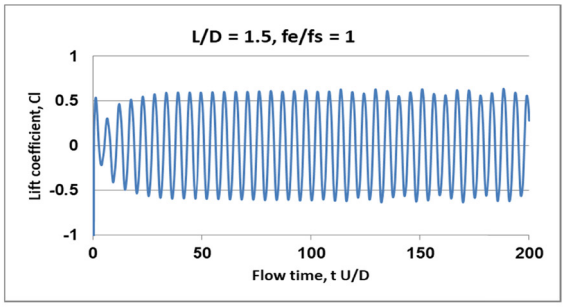

(c)

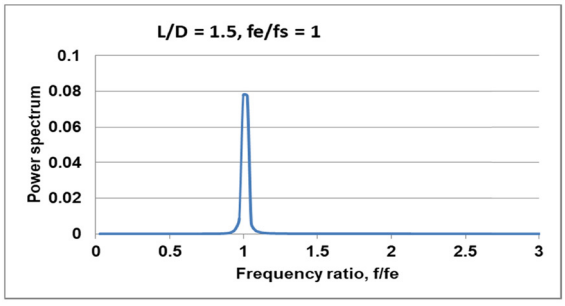

(d)

Figure 11: Lift coefficients' time history and power spectrum diagram of the downstream cylinder, L/D = 1.5 and Re = 200. (a) and (b) for f_e/f_s = 0.8, (c) and (d) for f_e/f_s = 1.0, and (e) and (f) for f_e/f_s = 1.2.

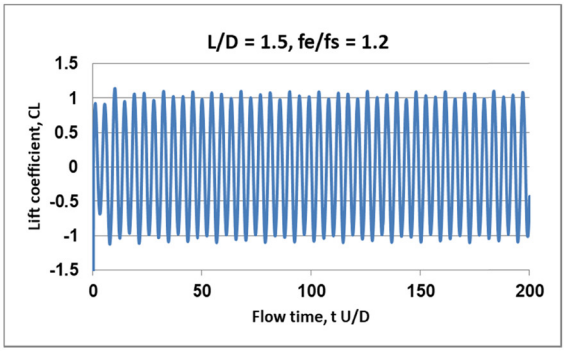

(e)

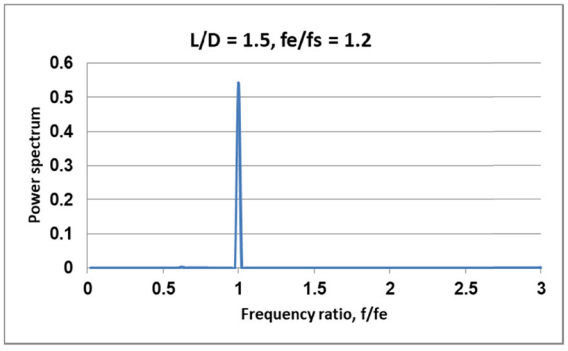

(f)

Figure 11: (*Continued*)

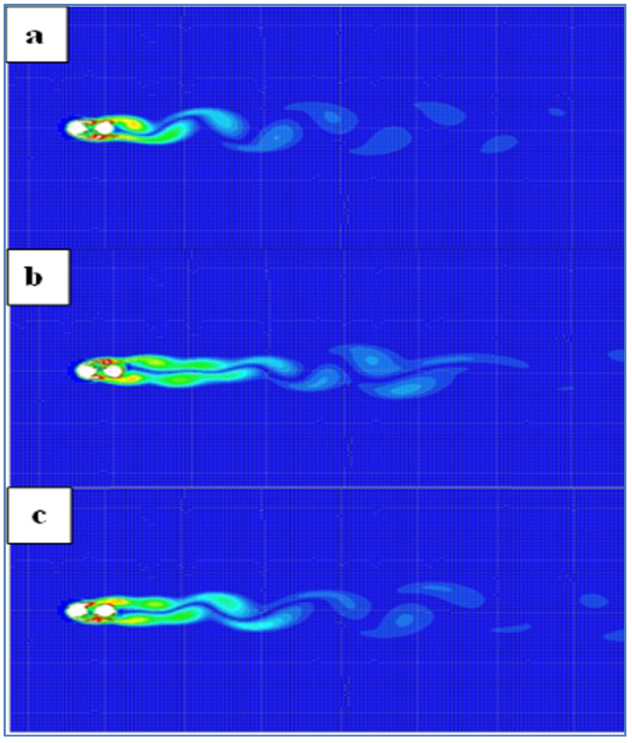

Figure 12: Instantaneous vorticity fields over the two vibrating cylinders, L/D = 1.5. (a) f_e/f_s = 0.8, (b) f_e/f_s = 1.0, and (c) f_e/f_s = 1.2.

corresponding to the cylinder excitation frequency f_e (dominant peak at f/f_e = 1.0). It can be concluded that the lock-in state for the case of spacing L/D = 1.5 occurs within a broader frequency range compared to the case of the single vibrating cylinder.

The vorticity fields over the two cylinders for the case L/D = 1.5 are shown in Figure 12. A clear 2 S mode vortex shedding around the downstream cylinder is observed at f_e/f_s = 0.8, as shown in Figure 12a. However, at f_e/f_s = 1.0 and 1.2, the near-downstream cylinder wake exhibits 2S* mode while the far wake turns into 2S mode, as depicted in Figure 12b and c.

On the other hand, for the case of larger spacing L/D = 4, the lock-in state of two vibrating cylinders is only observed at frequency ratio f_e/f_s = 0.8. Figure 13a and b shows that at f_e/f_s = 0.8, the lift coefficients' time history for the downstream cylinder is purely sinusoidal, and only the excitation frequency is dominated in the power spectrum diagram. However, no lock-in is observed at frequency ratios f_e/f_s = 1.0 and 1.2, as the beating behavior appears in the time histories of lift coefficients for the downstream cylinder (Figure 13c and e). Two peaks (primary peak at f_e and secondary peak at f_m) are observed in the frequency spectrum diagram for each cylinder (Figure 13d and f). It can be concluded that the lock-in state for spacing L/D = 4 occurs in a narrower frequency range than the single vibrating cylinder.

The vorticity fields for the case L/D = 4 are shown in Figure 14. For the lock-in state at f_e/f_s = 0.8 (Figure 14a), a pure 2S* mode vortex shedding over the downstream cylinder is seen. For no lock-in state at f_e/f_s = 1.0 (Figure 14b), the vortex shedding over the downstream cylinder evolves from the 2S mode in the near wake to the 2S* mode in the far wake. While for no lock-in state at f_e/f_s = 1.2 (Figure 14c), the vorticity fields display a clear 2S mode vortex shedding around the downstream cylinder.

5 Conclusions

Numerical simulations have been performed to investigate the flow over two equal-sized tandem circular cylinders at Reynolds number Re = 200. Both cylinders are forced to oscillate transversely in phase. The excitation frequency of the cylinders is varied at f_e/f_s = 0.8, 1.0, and 1.2 with a constant value of the amplitude ratio A/D = 0.25. An overset mesh technique in ANSYS FLUENT 19.0 was used to perform numerical simulations on the flow around the moving cylinders. The simulation results show that the

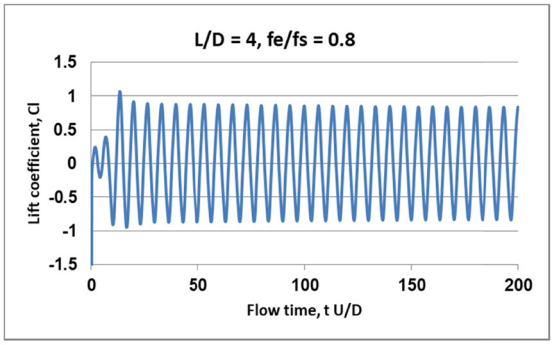

(a)

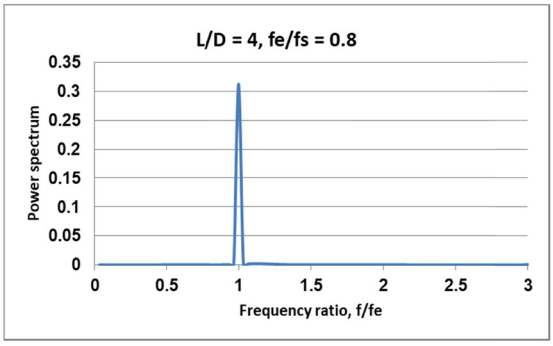

(b)

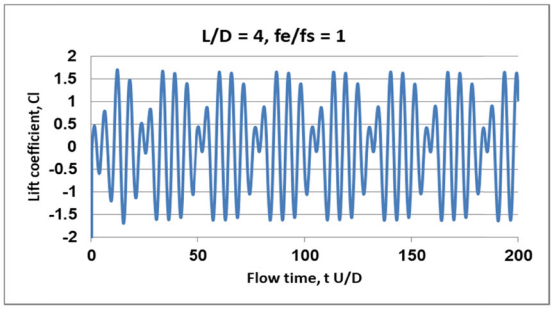

(c)

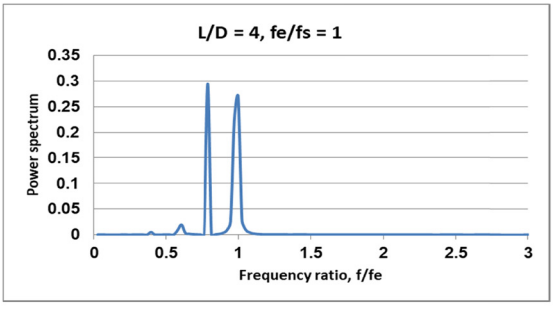

(d)

Figure 13: Lift coefficients' time history and power spectrum diagram of the downstream cylinder, L/D = 4 and Re = 200. (a) and (b) for f_e/f_s = 0.8, (c) and (d) for f_e/f_s = 1.0, and (e) and (f) for f_e/f_s = 1.2.

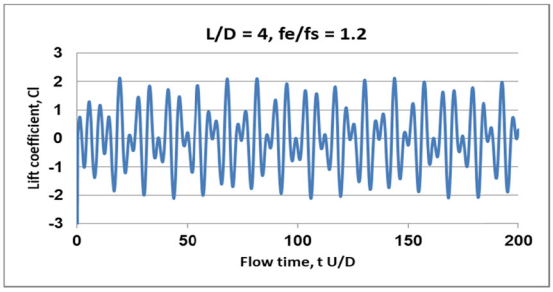

(e)

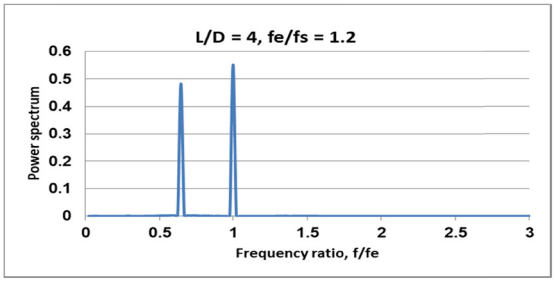

(f)

Figure 13: (*Continued*)

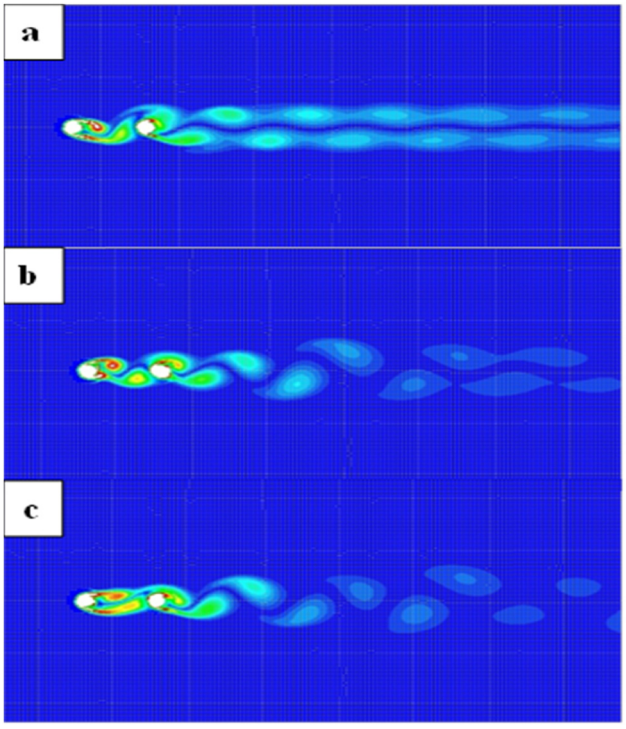

Figure 14: Instantaneous vorticity fields over the two vibrating cylinders, L/D = 4. (a) f_e/f_s = 0.8, (b) f_e/f_s = 1.0, and (c) f_e/f_s = 1.2.

spacing and vibration frequency affect the lock-in state of two vibrating cylinders. For the case of two vibrating cylinders with small spacing L/D = 1.5, the lock-in state appears for all frequency ratios f_e/f_s = 0.8, 1.0, and 1.2, while for larger spacing L/D = 4, the lock-in state is observed only for frequency ratio f_e/f_s = 0.8. In contrast, for the case of a single vibrating cylinder, the lock-in state occurs only for the frequency ratios f_e/f_s = 0.8 and 1.0. The vorticity fields for spacing L/D = 1.5 depict that the downstream wake modes are of clear 2S mode at low-frequency ratio f_e/f_s = 0.8, and a mixture of 2S* mode and 2S mode at higher frequency ratios f_e/f_s = 1.0 and 1.2. However, the downstream wake patterns for spacing L/D = 4 are 2S* mode at low-frequency ratio f_e/f_s = 0.8 and 2S mode at higher frequency ratios f_e/f_s = 1.0 and 1.2.

Funding information: The authors state no funding involved.

Author contributions: All authors have accepted responsibility for the entire content of this manuscript and approved its submission.

Conflict of interest: The authors state no conflict of interest.

References

[1] Bishop RED, Hassan AY. The lift and drag forces on a circular cylinder oscillating in a flowing fluid. Proc R Soc Lon A Math Phys Sci. 1964;277(1368):51–75.

[2] Koopmann GH. The vortex wakes of vibrating cylinders at low Reynolds numbers. J Fluid Mech. 1967;28(3):501–12.

[3] Tanida Y, Okajima A, Watanabe Y. Stability of a circular cylinder oscillating in uniform flow or in a wake. J Fluid Mech. 1973;61(4):769–84.

[4] Meneghini JR, Bearman PW. Numerical simulation of high amplitude oscillatory flow about a circular cylinder. J Fluids Struct. 1995;9:435–55.

[5] Nobari MRH, Naderan H. A numerical study of flow past a cylinder with cross flow and inline oscillation. Comput Fluids. 2006;35(4):393–415.

[6] Placzek A, Sigrist JF, Hamdouni A. Numerical simulation of an oscillating cylinder in a cross-flow at low Reynolds number: Forced and free oscillations. Comput Fluids. 2009;38(1):80–100.

[7] Kumar S, Navrose, Mittal S. Lock-in in forced vibration of a circular cylinder. Phys Fluids. 2016;28(11):1–15.

[8] Williamson CHK, Roshko A. Vortex formation in the wake of an oscillating cylinder. J Fluids Struct. 1988;2(4):355–81.

[9] Alawadhi EM. Numerical simulation of fluid flow past an oscillating triangular cylinder in a Channel. J Fluids Eng Trans ASME. 2013;135(4):1–10.

[10] Dekhatawala A, Shah R. Numerical investigation of two-dimensional laminar flow past various oscillating cylinder. Lecture Notes in Mechanical Engineering. Singapore: Springer; 2019. p. 261–71. doi: 10.1007/978-981-13-6416-7_25.

[11] Zdravkovich MM. The effects of interference between circular cylinders in cross flow. J Fluids Struct. 1987;1(2):239–61.

[12] Igarashi T. Characteristics of the flow around two circular cylinders arranged in tandem. Bull JSME. 1981;24(188):323–31.

[13] Li J, Chambarel A, Donneaud M, Martin R. Numerical study of laminar flow past one and two circular cylinders. Comput Fluids. 1991;19(2):155–70.

[14] Mittal S, Kumar V, Raghuvanshi A. Unsteady incompressible flows past two cylinders in tandem and staggered arrangements. Int J Numer Methods Fluids. 1997;25(11):1315–44.

[15] Sharman B, Lien FS, Davidson L, Norberg C. Numerical predictions of low Reynolds number flows over two tandem circular cylinders. Int J Numer Methods Fluids. 2005;47(5):423–47.

[16] Slaouti A, Stansby PK. Flow around two circular cylinders by the random vortex method. J Fluid Struct. 1992;6:641–70.

[17] Meneghini JR, Saltara F, Siqueira CLR, Ferrari Jr JA. Numerical simulation of flow interference between two circular cylinders in tandem and side-by-side arrangements. J Fluids Struct. 2001;15:327–50.

[18] Borazjani I, Sotiropoulos F. Vortex-induced vibrations of two cylinders in tandem arrangement in the proximity-wake interference region. J Fluid Mech. 2009;621:321–64.

[19] Sumner D, Wong SST, Price SJ, Païdoussis MP. Fluid behaviour of side-by-side circular cylinders in steady cross-flow. J Fluids Struct. 1999;13(3):309–38.

[20] Kang S. Characteristics of flow over two circular cylinders in a side-by-side arrangement at low Reynolds numbers. Phys Fluids. 2003;15(9):2486–98.

[21] Mahir N, Rockwell D. Vortex formation from a forced system of two cylinders part I: Tandem arrangement. J Fluids Struct. 1996;10(5):473–89.

[22] Papaioannou GV, Yue DKP, Triantafyllou MS, Karniadakis GE. Evidence of holes in the arnold tongues of flow past two oscillating cylinders. Phys Rev Lett. 2006;96(1):1–4.

[23] Versteeg H, Malalasekera W. An introduction to computational fluid dynamics: The finite volume method. 2nd ed. London, UK: Pearson Education; 2007.

[24] Al-Azawy MG, Turan A, Revell A. An overset mesh approach for valve closure: An LVAD application. Biodevices 2016 - 9th Int Conf Biomed Electron Devices, Proceedings; Part 9th Int Jt Conf Biomed Eng Syst Technol BIOSTEC 2016. 2016. Vol. 1 Biostec. p. 145–51.

[25] Hamdoon FO, Jaber AA, Flaieh EH. An overset mesh approach for a vibrating cylinder in uniform flow. Curved Layer Struct. 2022;9(1):396–402.

[26] Zhou CY, So RMC, Lam K. Vortex-induced vibrations of an elastic circular cylinder. J Fluids Struct. 1999;13(2):165–89.